Acta Crystallographica Section F
Structural Biology and Crystallization Communications
ISSN 1744-3091

Crystallization and preliminary crystallographic analysis of fragaceatoxin C, a pore-forming toxin from the sea anemone *Actinia fragacea*

A. E. Mechaly,[a] A. Bellomio,[b] K. Morante,[a] J. M. González-Mañas[a,c] and D. M. A. Guérin[a,c]*

[a]Unidad de Biofísica (CSIC–UPV/EHU), PO Box 644, E-48080 Bilbao, Spain, [c]Departamento de Bioquímica y Biología Molecular, Facultad de Ciencia y Tecnología, Universidad del País Vasco, PO Box 644, E-48080 Bilbao, Spain, and [b]Departamento de Bioquímica de la Nutrición, Instituto Superior de Investigaciones Biológicas, 4000 Tucumán, Argentina

Correspondence e-mail: diego.guerin@ehu.es

Received 30 January 2009
Accepted 25 February 2009

Sea anemones produce water-soluble toxins that have the ability to interact with cell membranes and form pores within them. The mechanism of pore formation is based on an initial binding step followed by oligomerization and membrane insertion. Although the final structure of the pore remains unclear, biochemical studies indicate that it consists of a tetramer with a functional radius of ∼1.1 nm. Since four monomers seem to be insufficient to build a pore of this size, the currently accepted model suggests that lipids might also participate in its structure. In this work, the crystallization and preliminary crystallographic analysis of two crystal forms of fragaceatoxin C (FraC), a newly characterized actinoporin from *Actinia fragacea*, are described. The crystals diffracted up to 1.8 Å resolution and the preliminary molecular-replacement solution supports an oligomeric structure of about 120 Å in diameter.

1. Introduction

Sea anemones produce two types of protein toxins: neurotoxins, which mainly act on ion channels (Honma & Shiomi, 2006), and cytolysins, which are also known as actinoporins (Anderluh & Maček, 2002). Actinoporins are cysteineless highly basic 20 kDa proteins (pI > 9.5) with pore-forming, haemolytic, cytotoxic and heart-stimulatory activities (Maček *et al.*, 1994; Anderluh & Maček, 2002). More than 30 different cytolysins have been described to date and they constitute the anemone_cytotox protein family of pore-forming toxins (Pfam code PF06369). Proteins belonging to this family show a high degree of sequence identity (between 60 and 85%) and sequence similarity (between 70 and 95%) (Alegre-Cebollada *et al.*, 2007). Two members of this family, equinatoxin II (Eqt-II) from *Actinia equina* and sticholysin II (Stn-II) from *Stichodactyla helianthus*, have been the subject of extensive research during the last decade and their three-dimensional structures have been solved by X-ray crystallography (Athanasiadis *et al.*, 2001; Mancheño *et al.*, 2003) and NMR (Hinds *et al.*, 2002). Both proteins consist of a β-sandwich core formed by ten (for Stn-II) or 12 (for EqT-II) β-strands flanked by two short α-helices. One of these α-helices is amphipathic and is located at the N-terminus. This helix seems to be able to detach from the main body of the molecule and participate in formation of the pore (Athanasiadis *et al.*, 2001).

Based on structural and biochemical results, a mechanism for pore formation has been proposed in which different regions of the protein seem to play crucial roles in each particular step (for a recent review, see Alegre-Cebollada *et al.*, 2007). Briefly, the toxin is secreted as soluble monomers which bind to the target membrane. The presence of sphingomyelin and/or the coexistence of lipid phases in the target membrane greatly enhance the affinity of cytolysins towards the membrane (Barlič *et al.*, 2004; Alegre-Cebollada *et al.*, 2006; Martínez *et al.*, 2007; Bakrač *et al.*, 2008; Schön *et al.*, 2008). The bound monomer then inserts its N-terminal amphipathic α-helix into the lipid membrane (Hong *et al.*, 2002; Malovrh *et al.*, 2003; Gutiérrez-Aguirre *et al.*, 2004; Kristan *et al.*, 2007). Since the functional pore is most likely to consist of four monomers (Belmonte *et al.*, 1993; Tejuca *et al.*, 1996; Mancheño *et al.*, 2003), oligomerization must take place at some stage during this process. However, it is not clear whether the

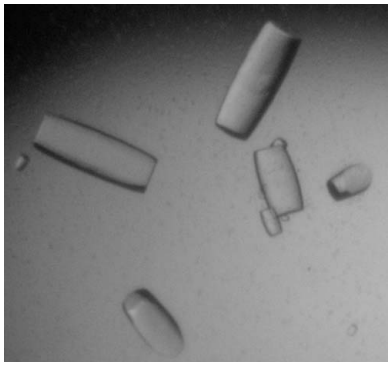

association of monomers takes place before, during or after the insertion process. The resulting pore has a functional radius of ~1.1 nm (Belmonte *et al.*, 1993; de los Ríos *et al.*, 1998; Tejuca *et al.*, 2001). As four monomers seem to be insufficient to build a pore of this size, the currently accepted model suggests that lipids might also participate in its structure (Alvarez *et al.*, 2001; Mancheño *et al.*, 2003; Malovrh *et al.*, 2003; Anderluh *et al.*, 2003).

Novel actinoporins have recently been isolated from the venom of *A. fragacea* (Bellomio *et al.*, 2009), a sea anemone which can be found on the lower shoreline of the northern rocky coast of Spain, as well as in the waters of the English Channel and southwest England (British Marine Life Study Society; http://www.glaucus.org.uk). One of them, fragaceatoxin C (FraC), has been purified to homogeneity, cloned and sequenced (Bellomio *et al.*, 2009). FraC has a molecular mass of 19.72 kDa and a theoretical pI of 9.57 (Bellomio *et al.*, 2009). In this work, we describe the crystallization and preliminary crystallographic analysis of two crystal forms of FraC, named type I and type II, that grow under the same conditions. Type I crystals diffracted to 1.8 Å resolution and the preliminary molecular-replacement solution indicates that FraC forms an oligomeric structure of about 120 Å in diameter.

2. Materials and methods

2.1. Purification

FraC was isolated from specimens of *A. fragacea* collected from the shoreline of the northern rocky coast of Spain, facing the Cantabrian sea and the Bay of Biscay. The purification protocol is described elsewhere (Bellomio *et al.*, 2009). It is largely based on the isolation of recombinant equinatoxin II (Anderluh *et al.*, 1996), which avoids the acetone-precipitation step described for the purification of natural equinatoxin II (Maček & Lebez, 1988). This method maintains the toxin in its native conformation and minimizes the protein loss that inevitably takes place after acetone precipitation.

2.2. Dynamic light scattering

Purified FraC at 6 mg ml^{-1} in 20 m*M* Tris–HCl pH 7.8 at 291 K was analyzed using ZetaSizer Nano-S dynamic light-scattering (DLS) equipment (Malvern). Prior to the measurements, protein samples were centrifuged for 10 min at 13 000*g* in an Eppendorf Mini Spin Plus centrifuge in order to remove possible aggregates. The measured hydrodynamic diameter of this solution was 4.2 nm (polydispersity index 0.240), corresponding to an estimated molecular mass of 19.1 kDa. This measurement confirmed that under these conditions FraC was present in the water-soluble monomeric form.

2.3. Crystallization

Initial crystallization screenings (192 conditions) were performed using the sitting-drop method in 96-well CrystalQuick plates, dispensing 200 nl drops using a Mosquito robot (TTP LabTech). Preliminary results performed at room temperature with a 1:1 mixture of protein solution (6 mg ml^{-1}) and 1.28 *M* sodium malonate, 0.11% LDAO pH 7.0 (condition G5 of the High Probability Salt Screen from Axygen Biosciences) gave very thin plate-shaped crystals. Starting from this initial result, we tested about 500 crystallization conditions using CrysChem plates, varying the parameters protein concentration (up to 20 mg ml^{-1}) and pH, using different detergents and concentrations and replacing sodium malonate by sodium formate. The optimal crystallization conditions were obtained at room temperature using 100–300 µl 4 *M* sodium formate (in 10 m*M* Tris pH 7.8) in the reservoir and drops made up of 3 µl 4–6 mg ml^{-1} FraC, 1 µl 0.33% LDAO and 2 µl reservoir solution. Typically, many crystals appeared in the drops within 3 d and reached maximum dimensions in approximately two weeks. Intriguingly, two crystal forms were obtained under the same crystallization conditions and the main difference between drops giving different crystal types was the maximum size and number of crystals within the drops (Fig. 1).

Since the mother liquor had a high cryosalt (sodium formate) concentration, no cryoprotection treatment was applied to the crystals. Both type I and type II crystals were mounted in a loop, cryocooled by plunging into liquid nitrogen, stored in magnetic vials and placed into a refrigerated canister (MDL) for transportation and transfer to the ESRF Robotic Sample Changer.

2.4. X-ray data collection and processing

Diffraction data were collected at 100 K under a nitrogen stream using synchrotron radiation on European Synchrotron Facility (ESRF) beamline ID14-4, Grenoble, France. A complete data set was

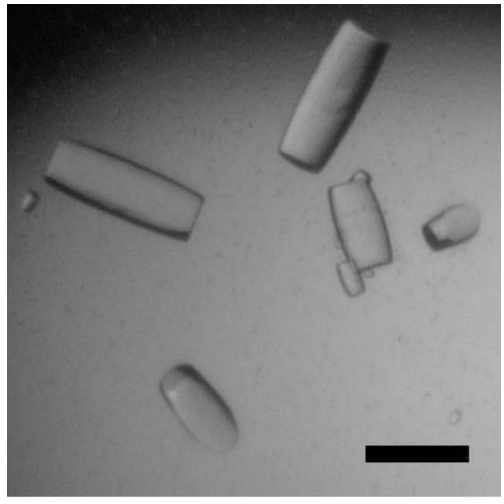

(*a*)

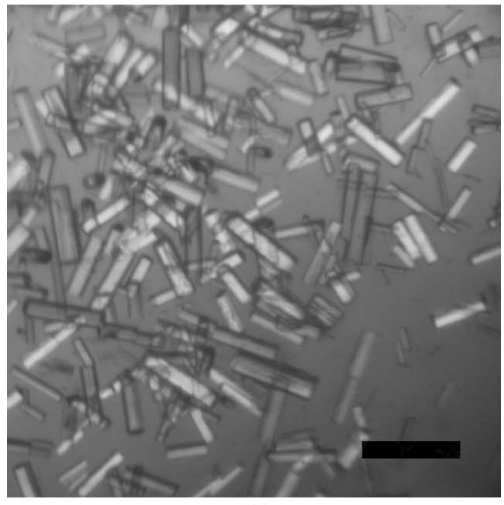

(*b*)

Figure 1
FraC crystals. FraC type I (*a*) and type II (*b*) crystals grew under the same crystallization conditions. Apart from the different size and number of crystals within the drops, type II crystals were twinned (see text). The two crystal types belonged to different space groups and the unit-cell parameter *c* was much longer in type II crystals than in type I crystals (see Table 1). The scale bars are 100 µm in length.

collected from a single crystal for each of the two crystal forms. For the type I crystal 720 frames were collected with an oscillation range of 0.25° (covering a total of 180°) and 0.5 s exposure time per image (Fig. 2). For the type II crystal a set of 360 frames were collected with an oscillation range of 0.5° and 0.5 s exposure time. Data were indexed and integrated with *MOSFLM* (Kabsch, 1993) and scaled with *SCALA* (Evans, 2005) from the *CCP*4 suite (Collaborative Computational Project, Number 4, 1994).

3. Results and discussion

Two types of FraC crystals were grown from the same crystallization conditions and complete data sets were obtained for both crystal types. A summary of the data-collection and processing statistics is shown in Table 1. A large difference in the unit-cell parameter *c* was observed between the two crystal types (Table 1).

The type II crystal belonged to space group *P*321 and according to tests performed with the programs *phenix.xtriage* (Adams *et al.*, 2002) and *SFCHECK* (Vaguine *et al.*, 1999), the data set presented perfect twinning (twinning law $-k$, $-k$, l).

A molecular-replacement solution was found for type I crystal data in space group $P6_322$, using a monomer of the crystal structure of EqT-II (Athanasiadis *et al.*, 2001; PDB code 1iaz) as a search model and employing the program *Phaser* (McCoy, 2007). The asymmetric unit contains six monomers and there are 72 monomers per unit cell (Z = 72). The solvent content is 57%, corresponding to a Matthews coefficient (V_M) of 2.87 Å^3 Da^{-1} (Matthews, 1968). A repeating crown-shaped motif is built when one of the crystallographic axis is applied to the asymmetric unit and all the crowns have the same size of about 120 Å in diameter (not shown). Although similar in size, this preliminary solution of the crystallographic FraC structure contrasts with the tetrameric model of the toroidal pore proposed for sticholysin II (Mancheño *et al.*, 2003). Refinement of the type I crystal structure of FraC is now in progress and the final model will be published in a forthcoming article.

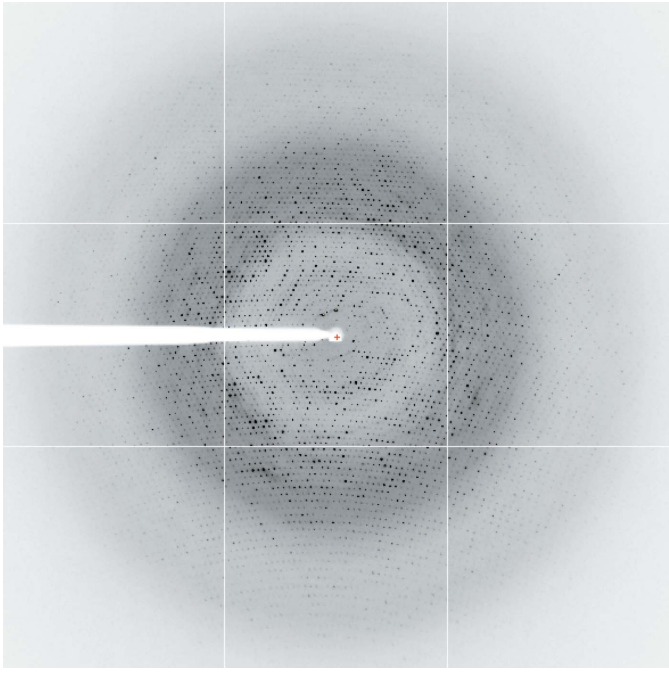

Figure 2
Diffraction image of a type I FraC crystal. The image corresponds to 0.5 s exposure time and 0.25° oscillation angle with a crystal-to-detector distance of 254 mm. Spots are visible at the detector edge, where the resolution is 1.8 Å. The image was obtained at ESRF, Grenoble (beamline ID14-4, wavelength 0.9795 Å) using an ADSC Quantum Q315r CCD detector.

Table 1
Data-collection statistics for type I and type II FraC crystals.

Values in parentheses are for the highest resolution shell.

	Type I	Type II
Beamline	ID14-4	ID14-4
Wavelength (Å)	0.9795	0.9795
Resolution (Å)	50.0–1.8 (1.90–1.80)	50.0–3.0 (3.16–3.00)
Space group	$P6_322$	$P321$
Unit-cell parameters (Å)		
$a = b$	117.90	118.535
c	343.23	430.664
Unique reflections	127597	69878
R_{merge} (%)	0.095 (0.569)	0.290 (0.522)
Completeness (%)	97.0 (94.6)	98.1 (98.1)
Multiplicity	15.3 (15.0)	3.1 (3.2)
$\langle I/\sigma(I)\rangle$	25.3 (4.1)	5.4 (1.8)

4. Conclusions

The diffraction data collected from the type I crystals reported in this work will provide sufficient information for the determination of the structure of the novel actinoporin FraC. This result will provide a wealth of information about the toxin oligomerization and will most likely give rise to a new structural model for the membrane-bound pore.

AEM and KM are the recipients of fellowships from the MICINN, Spain. AB is a staff scientist of the CONICET (Argentina) and was the recipient of a postdoctoral fellowship from the Basque Government. We also thank the ESRF for support for data collection as well as the members of the ID14-4 staff for assistance. Part of this work was funded by MEC (BFU2004-03452/02955). The work of DMAG was partially supported by the Bizkaia:Xede.

References

Adams, P. D., Grosse-Kunstleve, R. W., Hung, L.-W., Ioerger, T. R., McCoy, A. J., Moriarty, N. W., Read, R. J., Sacchettini, J. C., Sauter, N. K. & Terwilliger, T. C. (2002). *Acta Cryst.* D**58**, 1948–1954.
Alegre-Cebollada, J., Oñaderra, M., Gavilanes, J. G. & del Pozo, A. M. (2007). *Curr. Protein Pept. Sci.* **8**, 558–572.
Alegre-Cebollada, J., Rodríguez-Crespo, I., Gavilanes, J. G. & del Pozo, A. M. (2006). *FEBS J.* **273**, 863–871.
Alvarez, C. A., Serra, M. D., Potrich, C., Bernhart, I., Tejuca, M., Martínez, D., Pazos, F., Lanio, M. E. & Menestrina, G. (2001). *Biophys. J.* **80**, 2761–2774.
Anderluh, G. & Maček, P. (2002). *Toxicon*, **40**, 111–124.
Anderluh, G., Pungerčar, J., Štrukelj, B., Maček, P. & Gubenšek, F. (1996). *Biochem. Biophys. Res. Commun.* **220**, 437–442.
Anderluh, G., Serra, M. D., Viero, G., Guella, G., Maček, P. & Menestrina, G. (2003). *J. Biol. Chem.* **278**, 45216–45223.
Athanasiadis, A., Anderluh, G., Maček, P. & Turk, D. (2001). *Structure*, **9**, 341–346.
Bakrač, B., Gutiérrez-Aguirre, I., Podlesek, Z., Sonnen, A. F., Gilbert, R. J., Macek, P., Lakey, J. H. & Anderluh, G. (2008). *J. Biol. Chem.* **283**, 18665–18677.
Barlič, A., Gutiérrez-Aguirre, I., Caaveiro, J. M. M., Cruz, A., Ruiz-Argüello, M. B., Pérez-Gil, J. & González-Mañas, J. M. (2004). *J. Biol. Chem.* **279**, 34209–34216.
Belmonte, G., Pederzolli, C., Maček, P. & Menestrina, G. (1993). *J. Membr. Biol.* **131**, 11–22.
Bellomio, A., Morante, K., Barlič, A., Gutiérrez-Aguirre, I., Viguera, A. R. & González-Mañas, J. M. (2009). Submitted.
Collaborative Computational Project, Number 4 (1994). *Acta Cryst.* D**50**, 760–763.

de los Ríos, V., Mancheño, J. M., Lanio, M. E., Oñaderra, M. & Gavilanes, J. G. (1998). *Eur. J. Biochem.* **252**, 284–289.
Evans, P. (2006). *Acta Cryst.* D**62**, 72–82.
Gutiérrez-Aguirre, I., Barlič, A., Podlesek, Z., Maček, P., Anderluh, G. & González-Mañas, J. M. (2004). *Biochem. J.* **384**, 421–428.
Hinds, M. G., Zhang, W., Anderluh, G., Hansen, P. E. & Norton, R. S. (2002). *J. Mol. Biol.* **315**, 1219–1229.
Hong, Q., Gutiérrez-Aguirre, I., Barlič, A., Malovrh, P., Kristan, K., Podlesek, Z., Maček, P., Turk, D., González-Mañas, J. M., Lakey, J. H. & Anderluh, G. (2002). *J. Biol. Chem.* **277**, 41916–41924.
Honma, T. & Shiomi, K. (2006). *Mar. Biotechnol.* **8**, 1–10.
Kabsch, W. (1993). *J. Appl. Cryst.* **26**, 795–800.
Kristan, K., Viero, G., Maček, P., Dalla Serra, M. & Anderluh, G. (2007). *FEBS J.* **274**, 539–550.
Maček, P., Belmonte, G., Pederzolli, C. & Menestrina, G. (1994). *Toxicology*, **87**, 205–227.
Maček, P. & Lebez, D. (1988). *Toxicon*, **26**, 441–451.
Malovrh, P., Viero, G., Dalla Serra, M., Podlesek, Z., Lakey, J. H., Maček, P., Menestrina, G. & Anderluh, G. (2003). *J. Biol. Chem.* **278**, 22678–22685.
Mancheño, J. M., Martín-Benito, J., Martínez-Ripoll, M., Gavilanes, J. G. & Hermoso, J. A. (2003). *Structure*, **11**, 1319–1328.
Martínez, D., Otero, A., Álvarez, C., Pazos, F., Tejuca, M., Lanio, M. E., Gutiérrez-Aguirre, I., Barlič, A., Iloro, I., Arrondo, J. L. R., González-Mañas, J. M. & Lissi, E. (2007). *Toxicon*, **63**, 32–41.
Matthews, B. W. (1968). *J. Mol. Biol.* **33**, 491–497.
McCoy, A. J. (2007). *Acta Cryst.* D**63**, 32–41.
Schön, P., García-Sáez, A., Malovhr, P., Bacia, K., Anderluh, G. & Schwille, P. (2008). *Biophys. J.* **97**, 691–698.
Tejuca, M., Serra, M. D., Ferreras, M., Lanio, M. E. & Menestrina, G. (1996). *Biochemistry*, **35**, 14947–14957.
Tejuca, M., Serra, M. D., Potrich, C., Álvarez, C. & Menestrina, G. (2001). *J. Membr. Biol.* **183**, 125–135.
Vaguine, A. A., Richelle, J. & Wodak, S. J. (1999). *Acta Cryst.* D**55**, 191–205.